Near-source strong ground motions inferred from displaced geologic objects

Tamarah King[1], Mark Quigley[1] and Mike Sandiford[1]

1. School of Earth Sciences, University of Melbourne, Victoria, 3010.
Email: Tamarah.king@unimelb.edu.au

Abstract

Strong ground motions of the 2016 moment magnitude (M_w) 6.1 Petermann earthquake caused loose or semi-attached exfoliation sheets of granitic outcrops on the hanging-wall and foot-wall near the surface rupture trace to dislodge and travel up to 1m from their original locations. The direction, distance and method of movement were collected for 570 rock chips across 8 locations and 91 individual outcrops. Chip sizes range from <5cm up to 50cm width. Outcrops vary from <1m diameter and <10cm high above the surrounding land surface, to >20m in diameter and >10m high. Data were obtained across a central transect perpendicular to the surface rupture. Directions of chip movement at each outcrop show clear directivity effects related to fling-step, rupture directivity and transient shaking experienced in the 2016 earthquake. These data provide geological constraints for seismologic models of near-source strong ground motion directivity associated with fault rupture propagation.
Keywords: near-source ground motions, rupture directivity, fling, earthquake geology,

1. INTRODUCTION

The study of strong ground motion propagation, directivity, and magnitude is fundamentally important to earthquake hazard maps and engineering. Models for near-source strong ground motions on reverse faults predict higher magnitude shaking intensities on the hanging-wall, directivity of ground motions related to fault mechanics, and fling related motions due to permanent displacement of the hanging wall (Abrahamson and Somerville, 1996; Somerville et al., 1997). Quantification of these modelled ground motions with real data has proven difficult due to the lack of dense, near-source seismic arrays on faults that have ruptured in historic times (Abrahamson and Donahue, 2013).

Australian cratonic earthquakes offer a unique opportunity to study the near-source effects of strong ground motions on reverse faults. Historic earthquakes up to M_w 6.6 have occurred in remote arid Australia, notably Tennant Creek (NT), Meckering and Cadoux (WA), causing no harm to population and little to no damage to infrastructure. However, earthquakes of only M_w 5.4 or less have caused recorded damage to the land surface, bedrock outcrops and nearby landforms (Twidale and Bourne, 2000; Clark et al., 2014).

This paper explores how near-source strong ground motions affect local surface geology, as a proxy for direct waveform data. The direction and magnitude of directivity and fault fling effects are documented, and provide geological ground motion proxies to supplement seismological data in the poorly monitored and modelled near-field region.

2. PETERMANN EARTHQUAKE

Australia's most recent surface rupturing earthquake, and largest earthquake for 18 years, occurred on the 20th May 2016 near the Petermann Ranges of far SW Northern Territory (Fig. 1). The USGS report M_w 6.0 and depth of 10km, while Geoscience Australia report ML 6.1 with no depth estimate. Source parameters for the event from various sources are listed in Table 1. The earthquake was felt 115km away in Yulara (Uluru) and indigenous communities up to 250km away. The closest seismometer was located 166km to the west in Warrakurna, Western Australia.

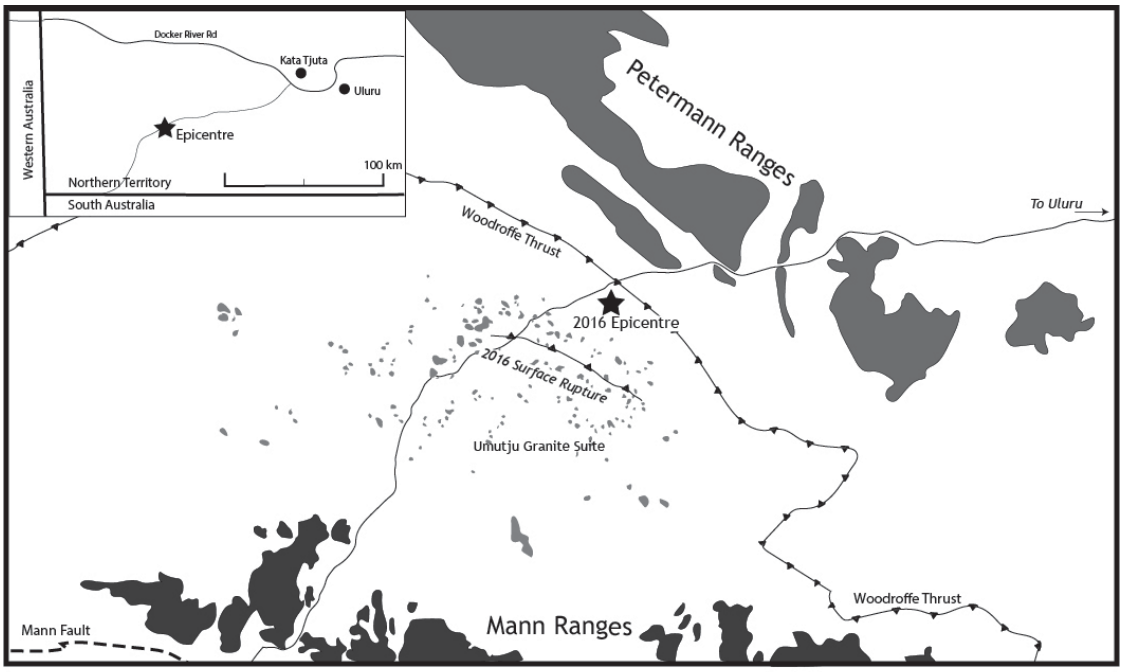

Figure 1. Location and geological context of Petermann Earthquake and fault scarp, 140km SW of Uluru. Petermann scarp dips north towards the large Neoproterozoic south dipping Woodroffe Thrust. Outcrops of granitic mylonite occur on the SW side of the Woodroffe Thrust, through which the 2016 event ruptured.

Table 1. Source parameters from various sources

Data location	Origin time	M_w	Depth	Datum	Latitude	Longitude	Phases	Strike1	Dip1	Rake1	Strike2	Dip2	Rake2	Scalar Moment
Geoscience Australia	18:14:02	6.1	0km	GDA	-25.579 ±6km	129.832 ±6km	87	-	-	-	-	-	-	-
USGS	18:14:04.67	6.0	10km ±1.7km	WGS	-25.566 ±2.2km	129.884 ±2.2km	330	140	38	97	312	52	85	-
GEOFON (Potsdam)	18:14:04.2	6.0	7km	WGS	-25.61	129.89	133	143	40	98	313	50	83	-
H. Ghasemi (GA)	18:14:02	6.1	20.9km	GDA	-25.56	129.88	15	137	26	105	300	65	83	2.15E+18 Nm
Global CMT	18:14:7.6	6.0	12km	WGS	-25.61	129.94	-	142	45	96	313	45	84	1.413E+25 Nm
D. Nadri (GA)	18:14:05.52	6.1	9.9km* ±9.8km	GDA	-25.628 ±12.2km	129.808 ±11.7km	-	-	-	-	-	-	-	

The Petermann Earthquake occurred on a north-dipping fault related to hanging-wall deformation of the south-dipping Neoproterozoic Woodroffe Thrust (Fig. 1). The 2016 surface rupture extends for ~18km NW-SE with an average vertical scarp offset of 0.2m and maximum offset of 0.96m.

The fault lies under red sand desert with longitudinal sand dunes up to 8m high trending roughly NW-SE. Sporadic low-lying outcrops of mylonite (<1m high) occur on clay pans and between dunes throughout the faulted area, while larger hills and outcrops (10-100m above dune fields) of granitic granulite/mylonite occur sporadically across the region. To the north and south of the faulted area are the Petermann and Mann Ranges with elevations averaging 200-500m above the dune fields and peaks up to 1000m.

Several large outcrops of unfoliated granitic mylonite on the hanging-wall and foot-wall of the 2016 earthquake experienced extensive gravitational rock damage attributed to coseismic strong ground motions (Fig. 2). Shaking effected steeply dipping exfoliation sheets on granite dome edges and large boulders/tors. Damaged and fallen rock were found to have crushed fresh vegetation, with fresh white dust at impact sites, and exposed weathering ‘shadows’ indicated dislodged boulders, sheet structures and loose chip movement.

Figure 2. Large outcrop damage to steeply dipping exfoliation sheets of large blocks, and steep outcrop edges.

Smaller sporadic outcrops of low-lying (<1m high) mylonite occur across the landscape on both hanging-wall and foot-wall including along the surface rupture itself (Fig. 3). In this arid environment the mylonite experiences chemical and physical weathering along exfoliation sheets more commonly than along foliation planes. Exfoliation sheets are generally 1-5cm thick and can be completely attached to the outcrop, semi-attached along edges, or completely detached but resting in place for considerable time. Exfoliation sheets partly shield the underlying outcrop from desert varnish formation and chemical weathering, creating ‘shadows’ of different coloured outcrop underneath.

Small exfoliation sheets and blocks (herein termed ‘chips’) were dislodged and transported from their original locations (identified by weathering ‘shadows’ and recent breakages) by strong ground motions. Chips ranged in size from <5cm width and 1cm thickness, up to dinner plate sized and 10cm thick. Very occasional large blocks of outcrop (>10kg) were observed offset from their original location. These chips flipped over, slid down-slope/dip or jumped across flat surfaces up to 1m from their original locations. Damaged and exposed vegetation, weathering shadows and recent breakages indicate the coseismic nature of movement.

Figure 3. Example of small outcrop of mylonite across the foot-wall and hanging-wall, typically flat to 1m high, showing visibly displaced exfoliation sheets (chips). Compass for scale and orientation.

3. DATA COLLECTION

Small outcrops observed during the 2016 field season occur in eight distinct locations along a transect roughly perpendicular to the surface rupture. Chip displacement data were collected from 91 separate outcrops across these eight locations, with 570 individual chips identified and recorded. Only 6% (n=44) of chip measurements were documented in the field due to time constraints, the other 94% were measured from GPS-located photographs.

Chips were photographed and moved around the outcrop to determine their original location. The shape of the chip, fresh breakage surfaces and weathering shadows on the outcrop were used to find the original location. Due to fieldwork time constraints, GPS-located photographs of outcrops were used to collect the majority of chip data by matching up shape and size of offset chips with erosional patterns and observably damaged areas. Data were collected to test whether chip morphology or rock type influenced the susceptibility to movement during rupture, and if there was a selection bias in direction of chip movement.

4. RESULTS

The locations of data across the transect are shown in Figure 4. The data for both hanging wall and foot wall are presented in Figure 5 as rose diagrams showing the number of chips per 10° bearing interval, and the average distance travelled per 10° bearing increment. These data were filtered to 403 measurements, with 167 chip displacements excluded based on low confidence of recentness of movement, and poorly identified original outcrop location.

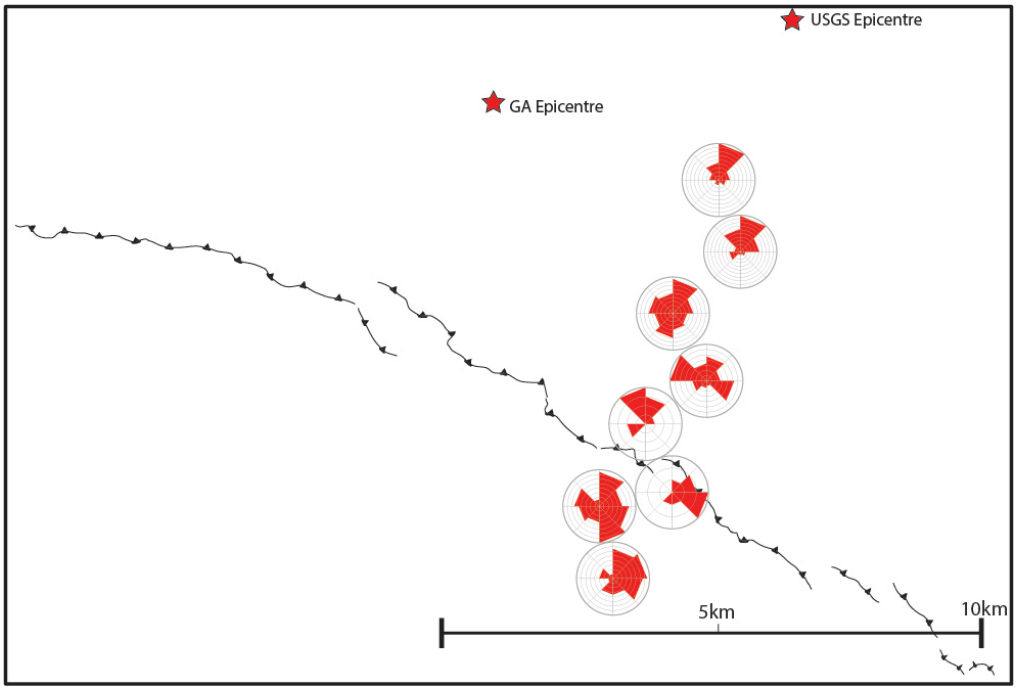

Figure 4. Location of central transect

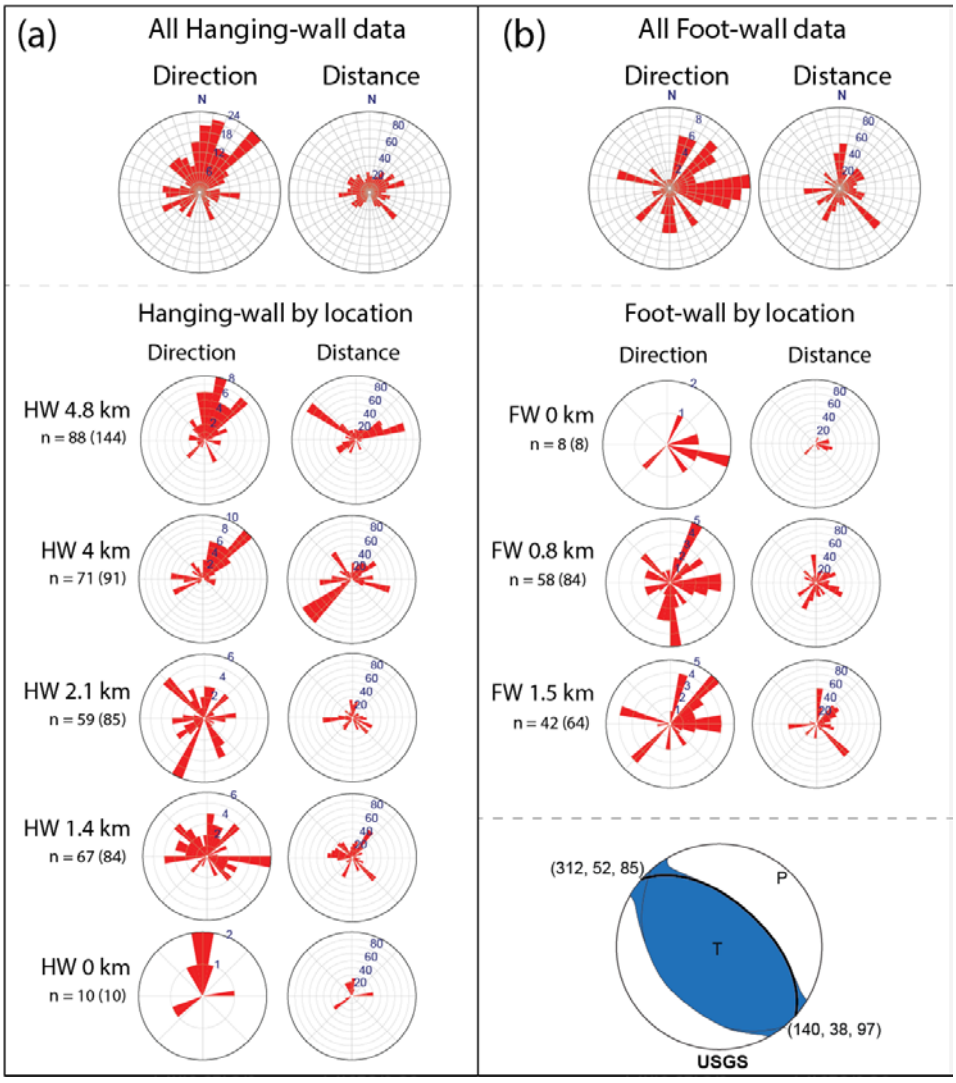

Figure 5. Rose diagrams for each of the eight locations across a fault-perpendicular central transect (a) hanging wall locations (b) footwall locations

5. DISCUSSION

Strong ground motion directivity effects are evident across the transect, with hanging-wall chip displacements moving predominately in a NE direction and foot-wall chip displacements towards the east. Patterns of movement vary across the hanging-wall with fault perpendicular signals becoming balanced by fault parallel displacements closer to the surface rupture.

Fault perpendicular chip displacements, with vectors orientated away from the surface rupture, are thought to relate to fling-step effects. This near-source ground motion results from permanent static ground displacement due to fault offset, and has been characterised by various authors (Somerville, 2002; Bray and Rodriguez-Marek, 2004; Burks and Baker, 2016). In the Petermann earthquake, the hanging-wall ground surface and outcrops displaced SW while footwall outcrops and ground was displaced NE, leaving semi-attached and detached chips in their original positions to the NE (hanging-wall) and SW (foot-wall) (Fig. 6). Fling-step related chip displacement on the Petermann foot-wall is less clearly defined, this may relate to the majority of offset occurring on the hanging-wall, with minimal downward movement of the foot-wall. Footwall displacements may also preserve a dextral sense of rupture, though more data is required to adequately validate this pattern.

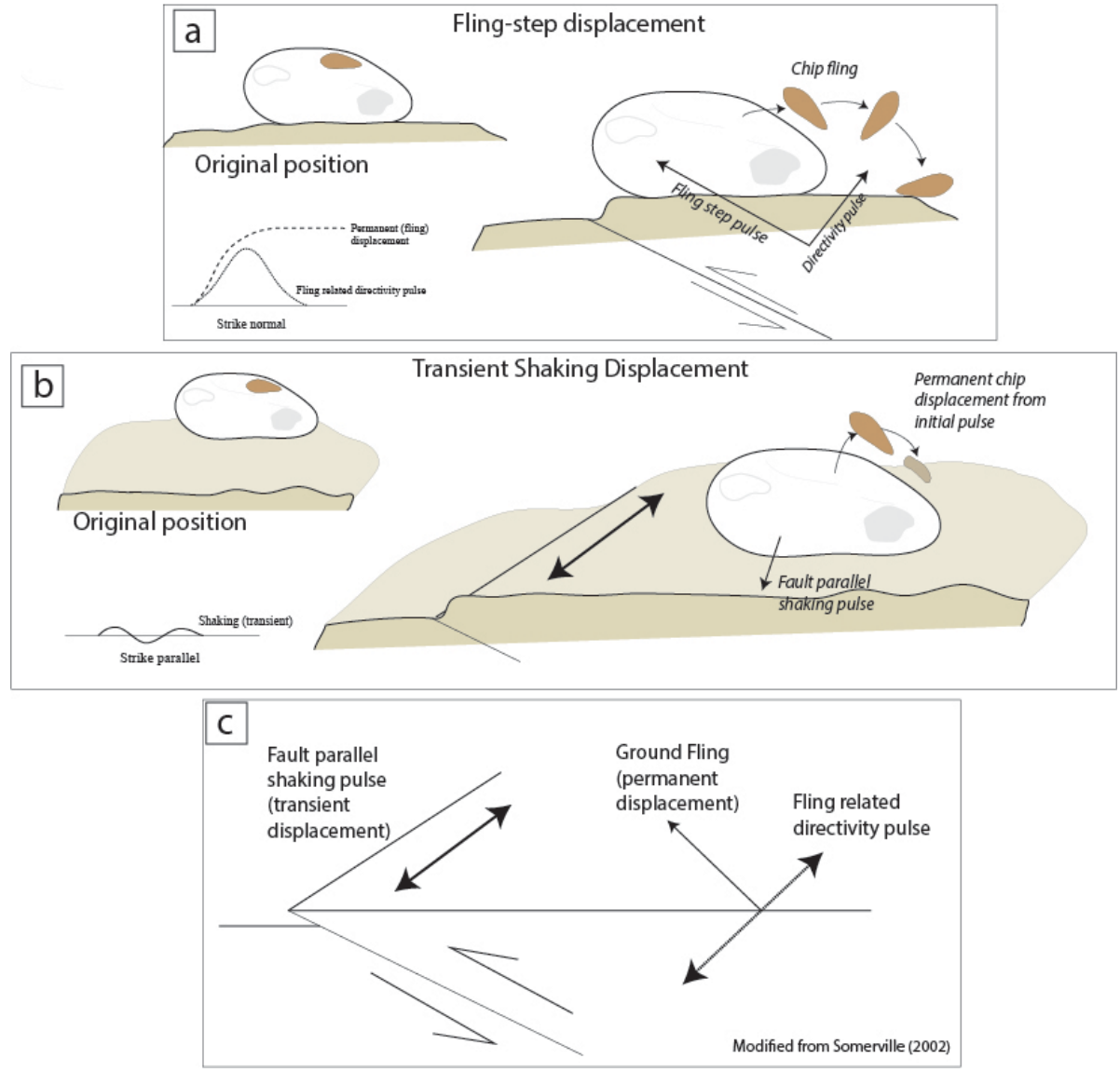

Figure 6. Schematic showing (a) permanent fling related chip movement perpendicular to fault orientation (b) transient shaking related chip movement parallel to fault orientation (c) models for dip-slip directivity ground motion pulses modified from Somerville (2002)

Somerville (2002) suggests that the dynamic rupture directivity pulse for reverse faults is fault normal, which in the case of the Petermann earthquake is NE, the direction of predominate chip displacement. It is likely that hanging-wall NE chip displacement is a combination of fling-step and directivity pulse, while SW movement of hanging-wall chips may preserve purely fling-step motions. Fling-step and fault directivity pulses are difficult to distinguish in traditional waveform data (Bray and Rodriguez-Marek, 2004). More chip displacement data, including analysis and modelling of the method of movement (flipped vs jumped) is required to understand if these ground motions are preserved by geological damage.

Fault parallel chip movements are thought to occur due to transient shaking displacement concurrent with and/or after the initial fault rupture offset and permanent ground displacement.

Hanging-wall outcrops at 2.1km and 1.4km have more diffuse displacement data, with a tendency towards fault parallel movement. This signal is attributed to transient ground motions resulting from S-wave propagation. These outcrops may have experienced complicated ground motions related to sub-surface fault-parallel lineaments, identified from a PALSAR2 wrapped interferogram (Fig. 7). Wave interference due to the tapering hanging-wall wedge may also have complicated chip displacement fields in the near-fault (<2km) region.

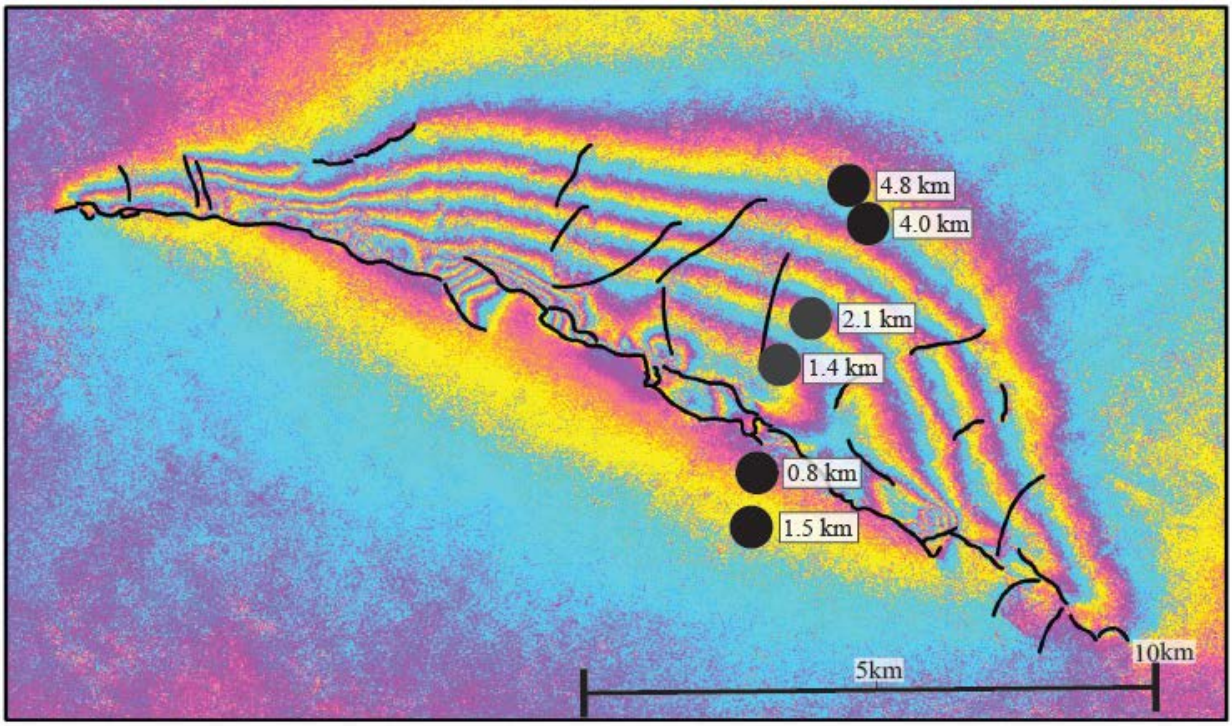

Figure 7. PALSAR2 wrapped interferogram with lineaments identified from coherence properties (pers comms. S. Lawrie, Geoscience Australia) with locations from this paper shown.

The majority of outcrops are flat to the ground or very low (79%). Those that do dip are predominately orientated NE in the direction of the fault itself. Though this may predispose some chips to gravity driven NE movement, the majority of chips (63%) are classified as having travelled horizontally or upslope, with no down-dip component of movement. This, combined with the lack of relationship between footwall outcrops dip direction and travel direction, suggests that the predominate control on chip movement is strong ground motion, not outcrop dip or gravity.

6. CONCLUSION

Displaced chips in the near-source region of the 2016 Petermann earthquake demonstrate offset related to fling-step, fault directivity and transient shaking effects. This study contributes a new geological dataset to near-source directivity measures and models. Near-source directivity recordings are lacking in seismology due to the sparseness of most seismic recording arrays, and difficulties in distinguishing fling step and fault directivity in near-source wave form data. This data demonstrate the applicability of geological damage to seismic models for fault rupture complexity, including near-source engineering problems.

REFERENCES

ABRAHAMSON, N.A., AND SOMERVILLE, P.G. 1996. Effects of the hanging wall and footwall on ground motions recorded during the Northridge earthquake. *Bulletin of the Seismological Society of America* **86**, 93–99.

BRAY, J.D., AND RODRIGUEZ-MAREK, A. 2004. Characterization of forward-directivity ground motions in the near-fault region. *Soil Dynamics and Earthquake Engineering* **24**, 815–828.

BURKS, L.S., AND BAKER, J.W. 2016. A predictive model for fling-step in near-fault ground motions based on recordings and simulations. *Soil Dynamics and Earthquake Engineering* **80**, 119–126.

CLARK, D., MCPHERSON, A., ALLEN, T.I., AND DE KOOL, M. 2014. Coseismic surface deformation caused by the 23 March 2012 Mw 5.4 Ernabella (Pukatja) earthquake, central Australia: Implications for fault scaling relations in cratonic settings. *Bulletin of the Seismological Society of America* **104**, 24–39.

SOMERVILLE, P.G. 2002. Characterizing Near Fault Ground Motion For The Design And Evaluation Of Bridges. *Proceedings of 3rd National Seismic Conference and Workshop on Bridges and Highways* 1–12.

SOMERVILLE, P.G., SMITH, N.F., GRAVES, R.W., AND ABRAHAMSON, N.A. 1997. Modification of Empirical Strong Ground Motion Attenuation Relations to Include the Amplitude and Duration Effects of Rupture Directivity. *Seismological Research Letters* **68**, 199–222.

TWIDALE, C.R., AND BOURNE, J.A. 2000. Rock bursts and associated neotectonic forms at Minnipa hill, northwestern Eyre Peninsula, South Australia. *Environmental and Engineering Geoscience* **6**, 129–140.